NAL TR-412T

UDC 539.43:
519.28:
620.178.3:
669.715.

TECHNICAL REPORT OF NATIONAL AEROSPACE LABORATORY

TR-412T

Relationship Between Scatter of Fatigue Life and S-N Curve of 2024-T4 Aircraft Structural Aluminum Alloy Specimens with a Sharp Notch (K_t=8.25) Under a Constant Temperature and Humidity Condition

Toshiyuki SHIMOKAWA and Yasumasa HAMAGUCHI

October 1977

NATIONAL AEROSPACE LABORATORY

CHŌFU, TOKYO, JAPAN

Relationship between Scatter of Fatigue Life and S-N Curve of 2024-T4 Aircraft Structural Aluminum Alloy Specimens with a Sharp Notch (K_t = 8.25) Under a Constant Temperature and Humidity Condition*

By

Toshiyuki SHIMOKAWA** and Yasumasa HAMAGUCHI**

ABSTRACT

This paper presents an investigation of the relationship between fatigue life scatter and S–N curve from the standpoint of a kind of error theory. When a new factor serving like an error in applied stress is added to an identical condition under which an $S-N$ curve has been obtained, it produces a deviation from the expected fatigue life and the amount of the deviation depends on the slope of the $S-N$ curve. In this study, the accumulated effect of all factors producing fatigue life scatter, which is found in a fatigue test by nominally identical specimens subjected to nominally identical repeated stresses, is regarded as an error in applied stress. Equivalent stress is defined as the sum of applied stress and the error in applied stress. This concept is used for analyzing the results of a series of fatigue tests on 2024-T4 aircraft structural aluminum alloy specimens with a sharp notch (K_t = 8.25) under a constant temperature and humidity condition. The interrelationship between scatter of equivalent stress, $S-\tilde{N}$ curve, where $\tilde{N}$ is the median fatigue life, and fatigue life scatter is discussed.

It became clear that equivalent stresses are distributed in almost normal distribution and their standard deviation is nearly constant (0.256 to 0.375 kg/mm²) regardless of stress level, and that fatigue life distribution has a strong correlation to the slope and shape of $S-\tilde{N}$ curve.

概　　要

本研究は疲労寿命のばらつきと $S-N$ 曲線の関係を一種の誤差論の立場から検討したものである。ある一定条件下の疲労試験で得られた $S-N$ 曲線を考えてみると，この一定条件に対し，応力側の誤差に換算して考えることのできる因子が新たに加われば，これは当初に予想した寿命からの偏差を生みだし，この偏差大きさは $S-N$ 曲線の傾きと形状に依存することが容易に理解できる。そこで，疲労寿命のばらつきの原因として考えられる因子の効果すべてを総合し，設定応力の誤差に換算して考え，設定応力との和を換算応力と定義する。この考えをもとに，温度および湿度を一定にした実験室で，航空機構造用アルミニウム合金 2024-T4 の鋭い切欠き（K_t = 8.25）を有する板状試験片によって行った疲労試験の結果について，換算応力分布，中央 $S-N$ 曲線，および疲れ寿命分布の相互関係について調べた。

この結果，換算応力の分布形はほぼ正規分布であり，標準偏差も応力によらず，ほぼ一定（0.256～0.375 kg／mm²）であった。このため，疲労寿命分布は中央 $S-N$ 曲線の傾きと形状に大きく影響されていると結論された。

* Received Aug. 12, 1977

** Second Airframe Division

Published in Journal of the Japanese Society for Strength and Fracture of Materials, Vol. 10, No. 2, 1975 and NAL TR-412, 1975 in Japanese.

1. INTRODUCTION

The fact that the scatter of fatigue life is much greater than those of other mechanical properties obtained by static tests has been known for a long time. To find out an appropriate distribution function of fatigue life of structural materials is one of the most important problems for probabilistic design and analysis of engineering structures. However, not so many tests the purpose of which is to investigate the fatigue life scattering properties have been carried out. This paper attempts to clarify the distribution property of fatigue life by considering the effect of an $S-N$ curve from the standpoint of a kind of error theory.

The factors which produce the scatter of fatigue life obtained by laboratory tests may be divided into the following three groups.

1) The factors depending on the manufactural irregularities of specimens tested and the random variations in the experimental conditions.
2) The factors depending on the inherent material variability.
3) The factors depending on the probabilistic nature of cumulative damage in fatigue process[1].

When a new factor serving like an error of applied stress is added to an identical condition under which an $S-N$ curve has been obtained, it produces a deviation from the expected fatigue life, and the amount of the deviation depends on the slope of the $S-N$ curve. The effect of most factors belonging to the groups of 1) and 2) may be estimated in an error of applied stress. Therefore, the amount of the deviation produced by these factors should depend significantly on the slope of the $S-N$ curve at the applied stress level. This concept suggests that the slope and shape of the $S-N$ curve should have a great effect on the scatter and distribution shape of fatigue life. There appears to have been no other researches considering the importance of an $S-N$ curve for the scattering property of fatigue life than those reported by the authors[2] and Matolcsy[3]. The latter investigated the relationship between fatigue life scatter and median fatigue life, assuming the error in load level to be constant.

In laboratory tests, any one of the three groups is not concluded to be the most important for the scatter of fatigue life. However, for specimens with a sharp notch, whose fatigue life is mostly covered by the crack propagation period, the test results by Tanaka et al.[4] showed the effect of the group 3) to be minor. Taking these facts into consideration, the authors tried to make fatigue life scatter in this experiment as small as possible by using the following methods. The temperature and humidity in the laboratory were kept constant in order to reduce the effect of a factor in the group 1). Sharp notched specimens were selected for this investigation, because the effect of the group 3) in such specimens has been shown to be small. And other various experimental techniques were introduced to decrease the scatter of fatigue life. Under these experimental conditions, the distribution of fatigue life and the crack initiation period were obtained.

The experimental results are analyzed in the following steps. The accumulated effect of all the factors producing the fatigue life scatter described above is regarded as an error in applied stress. Equivalent stress is defined as the sum of applied stress and the error in applied stress. An $S-\tilde{N}$ curve, where $\tilde{N}$ is the median fatigue life, is drawn from the experimental results. Then, the equivalent stress which corresponds to each fatigue life obtained in the test can be calculated by the $S-\tilde{N}$ curve and the fatigue life. The scatter and distribution shape of equivalent stress are evaluated. This evaluation provides the information as to how much scatter and what distribution shape of the error in applied stress are required to produce the fatigure life distribution obtained in the tests on the engineering standpoint. On the other hand, an equivalent stress distribution model is assumed by considering the experimental results. The fatigue life distribution is calculated from this model and the $S-\tilde{N}$ curve. The distribution property of fatigue life for the variation of the slope and shape of the $S-\tilde{N}$ curve is also discussed.

2. SPECIMENS AND TESTING PROCEDURE

The material of the specimens was 2024-T4 aircraft structural aluminum alloy sheet material in the unclad condition. The chemical composition and the mechanical properties are given in Table 1.

All the specimens were cut from two sheets of the same batch. The nominal thickness was 1 mm. The

Table 1 Chemical composition and mechanical properties of the material 2024-T4 used

Chemical composition	Cu	Si	Fe	Mn	Mg
Content (%)	4.39	0.17	0.32	0.50	1.30

Tensile strength kg/mm²	Yield stress (0.2% offset) kg/mm²	Elongation %	Young's modulus kg/mm²
51.1	38.6	20	7.35×10^3

specimen configuration is shown in Fig. 1. Their longitudinal direction were coincided with the grain direction. The specimens were first cut to their rectangular form with a slight oversize. Then the edges were milled to the accurate width and length of the specimens. The internal notch of the specimens was made by drilling in a jig, and the burrs attached around the hole were removed by light stoning. The theoretical elastic stress concentration factor in tension, K_t, is calculated as 8.25[5]. The specimens tested at one stress level were sampled randomly so as to exclude any bias on the results originating from the position of specimens in the sheet. Prior to testing, the specimens were simply degreased in Ethyl Alcohol and wiped dry with clean tissue.

Fatigue tests were performed on a conventional sub-resonant fatigue machine, operating at the frequency of 1,800 cycles per min. It is schematically illustrated in Fig. 2. All tests were carried out with a constant load amplitude by only one fatigue machine. The specimens were loaded on fully reversed plane bending by a four point bending fixture. Because this machine was driven by a synchronous motor, some overloads were originally observed during several seconds after the machine was set in motion. In order to prevent these overloads, a flywheel of about 2.4 kg was attached directly to the motor and a brake was used during several seconds after the machine was switched on. The overloads were completely removed by these devices. The synchronous motor was driven by the electricity of constant frequency and voltage supplied from a special power source equipment including a quartz oscillator.

The temperature and relative humidity in the laboratory were kept within the ranges 22 to 24°C and 50 to 56% respectively. Record samples of the temperature and relative humidity at about 50 cm apart from the specimen being tested are shown in Fig. 3. Such difference as between (a) and (b) in Fig. 3 was due to the air conditioning method. Namely, electric heaters, a refrigerator, a humidifier and a dehumidifier were used properly according to the season.

3. TEST RESULTS

3.1 Damage Curve Represented by Fatigue Crack Propagation

To get the percentage of fatigue life covered by fatigue crack initiation period and the behavior of its propagation, the damage curve represented by fatigue crack propagation was investigated. Fatigue damage accumulated in a specimen, D, is defined as Eq. (1).

$$D = \frac{\ell - \ell_o}{\ell_f - \ell_o} \quad \cdots\cdots\cdots\cdots\cdots\cdots \quad (1)$$

where ℓ_f is the specimen width, ℓ_o is the notch length, and ℓ is crack length, i.e., the sum of the notch length and true crack length. True crack length is defined as the average crack length on both sides of the specimen surface. The replica of the specimen surface at arbitrary number of cycles n was taken by using a thin plastic film. Crack length on the replica was measured through a 200 times magnification microscope. The relation of the damage D and the cycle ratio n/N is shown in Fig. 4, where N is the number of cycles to failure. Fig. 4 shows that a crack initiated in the first 5 percent of fatigue life

when an applied stress was higher than or equal to 8 kg/mm². About 30 percent of fatigue life was covered with the crack initiation period at the applied stress 7 kg/mm². Hence, it became clear that a fatigue life distribution was mostly determined by the scatter of crack propagation when an applied stress was higher than or equal to 8 kg/mm², while it depended on both scatters of crack initiation and propagation when an applied stress was equal to or lower than 7 kg/mm².

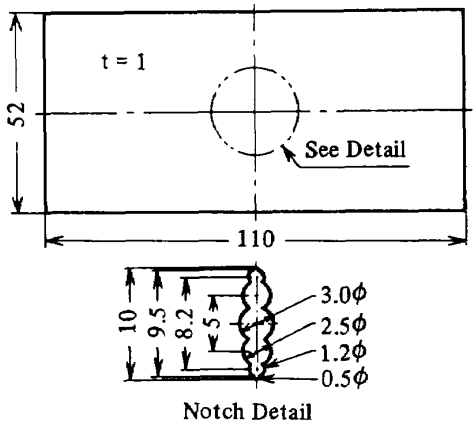

Fig. 1 Dimensions of specimens in millimeters, $Kt = 8.25$

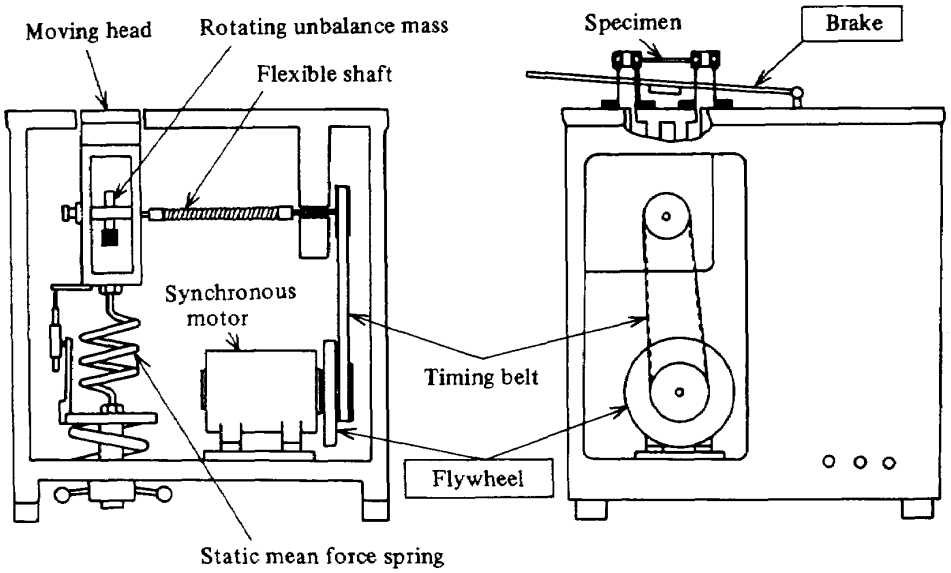

Fig. 2 Schematic view of the testing machine

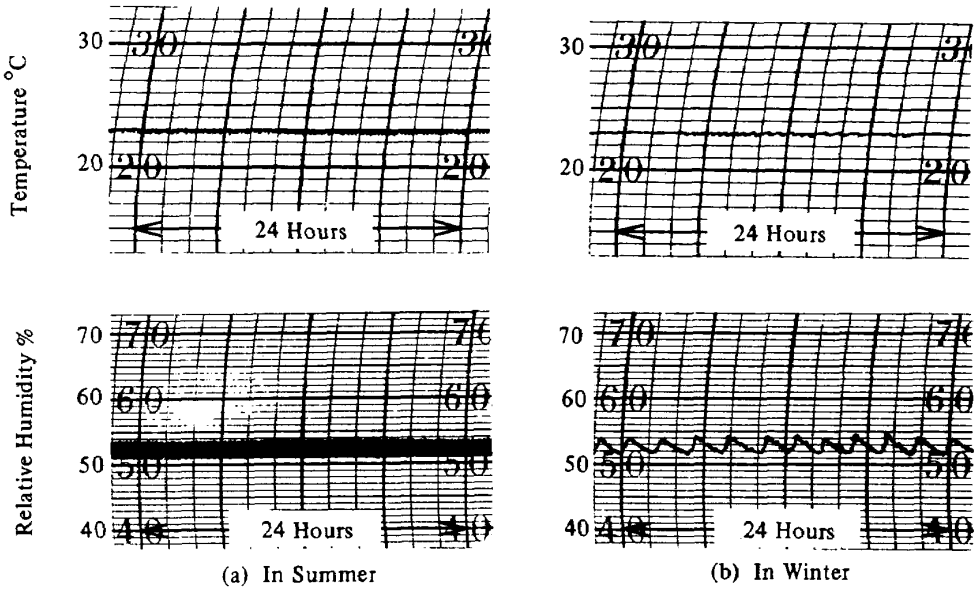

Fig. 3 Record samples of temperature and relative humidity in the laboratory

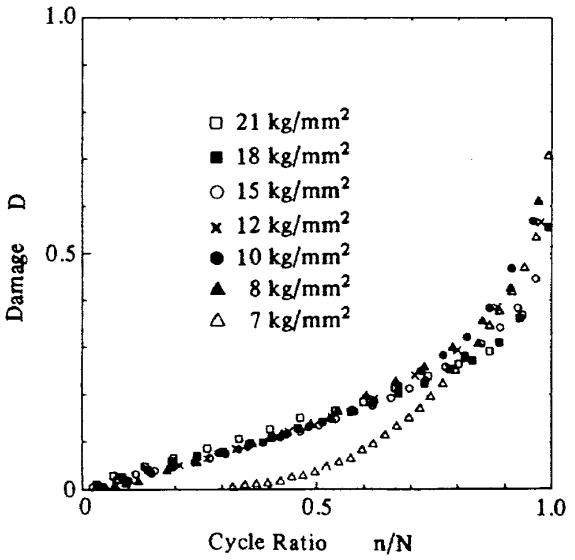

Fig. 4 Cycle ratio versus damage curves represented by fatigue crack propagation

3. 2 Fatigue Life Distribution and Its Statistical Parameters

Fatigue life tests were conducted at nine stress levels, which were 6.5, 7, 8, 10, 12, 15, 18, 21 and 22 kg/mm². For every stress level series, each specimen was tested using the appropriate load to give the same nominal stress. The test results of fatigue life N are given in Table 2 and shown in Fig. 5, plotting on log-normal probability paper. The series of tests stressed at 6.5 and 22 kg/mm² were performed to determine both external portions of the S–$\tilde{N}$ curve in the range of $S = 7 \sim 21$ kg/mm², where $\tilde{N}$ is the median fatigue life. Hence, the number of specimens tested at these stress levels was smaller than that at other stress levels, and the tests at 6.5 kg/mm² were truncated at 13,000,000 cycles. Statistical parameters computed from the test results of Table 2 are presented in Table 3. The plotting method used in this paper is the median ranks proposed by Johnson[6]. The median ranks are selected for the following three reasons. First, the distribution of order statistics is not necessarily symmetric. Second, when the distribution of order statistics transformed by some function, the median of original order statistics is transformed to the median of new ones. Finally, the median fatigue lives, $\tilde{N}$, are used to draw an S–N curve in a later section. Johnson has given the median rank table in Ref. (6) up to only sample size 20, so the median ranks used were calculated by the computer program of incomplete Beta function in Ref. (7). Fig. 5 shows that the distribution shape of fatigue life is practically log-normal at high stress levels $S = 10 \sim 22$ kg/mm², whereas it departs from the log-normal type at lower stress levels $S = 6.5 \sim 8$ kg/mm². The coefficient of variation of life, V_N, and the sample standard deviation, i.e., the square root of unbiased variance, of log-life, σ_L, are commonly used as an index of the scatter of fatigue life. Their values in Table 3 are small and nearly constant for higher stress range $S = 15 \sim 22$ kg/mm². Their values become larger as an applied stress is decreased lower than $S = 15$ kg/mm². The values of V_N and σ_L in Table 3 are much smaller than many other fatigue test results[8), 9), 10), 11), 12), 13), 14), 15), 16), 20)] and nearly equal to those in Ref. (17). It proves that the desired experimental results, i.e., small fatigue life scatters, were obtained.

As presented in Fig. 4, a crack grew throughout most of the whole life, when an applied stress was higher than or equal to 8 kg/mm². While, a fatigue life was covered with crack initiation and propagation periods, when an applied stress was not higher than 7 kg/mm². However, Fig. 5 shows that there was no remarkable difference in fatigue life distributions between the two stress ranges.

4. ANALYSIS OF TEST RESULTS AND DISCUSSION

4. 1 S–$\tilde{N}$ Curve's Equation

As shown in the preceeding section, there is the scatter in experimental fatigue lives and their distribution shape is not necessarily symmetric. Hence, the standard S–N curve is drawn from the median fatigue lives, $\tilde{N}$, in Table 3. The S–$\tilde{N}$ curve fitted to the experimental S–$\tilde{N}$ relations by eye is shown in Fig. 6.

The analytical expression of the S–$\tilde{N}$ curve is required for the later analysis and discussions of the test results. A good S–$\tilde{N}$ curve approximating sufficently to the experimental data could not be obtained by only one equation over the test stress range. In order to get a sufficient degree of approximation, S–$\tilde{N}$ curve's equations are determined separately around each stress level at which fatigue tests were carried out. S–$\tilde{N}$ curve's equation around an aimed stress level, which is one of the test stress levels,

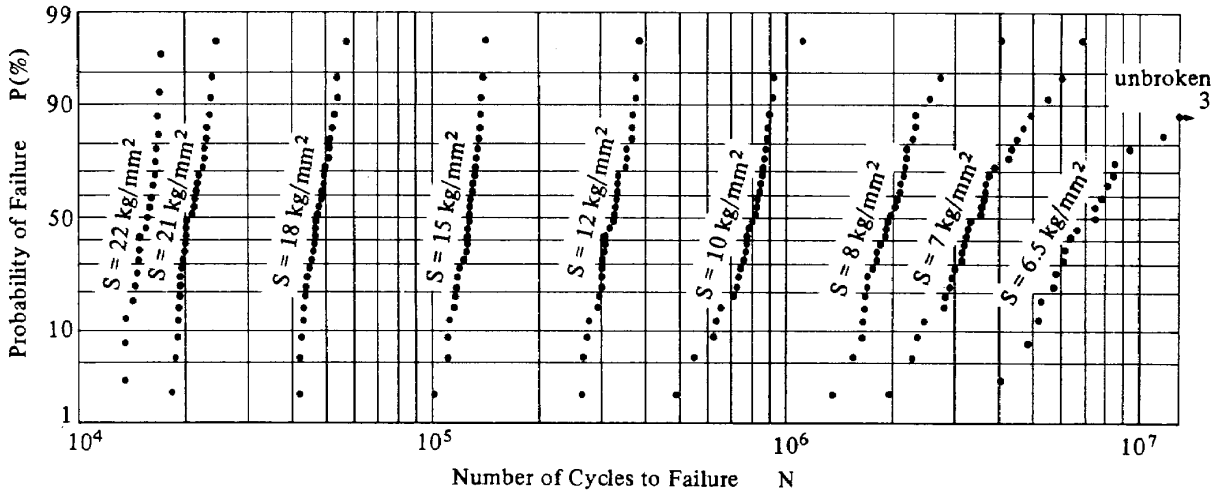

Fig. 5 Fatigue life distributions of Table 2

Table 2 Experimental data of fatigue life

No.	Stress S 22kg/mm²	Stress S 21kg/mm²	Stress S 18kg/mm²	Stress S 15kg/mm²	Stress S 12kg/mm²	Stress S 10kg/mm²	Stress S 8kg/mm²	Stress S 7kg/mm²	Stress S 6.5kg/mm²
1	13,600	18,400	42,100	101,600	265,200	490,500	1,351,300	1,958,700	4,037,200
2	13,600	18,900	42,300	111,000	266,100	545,100	1,546,000	2,280,700	4,822,400
3	13,700	19,100	42,700	111,000	273,500	623,100	1,646,800	2,356,700	5,162,300
4	14,400	19,200	43,100	112,000	276,900	634,500	1,649,700	2,461,000	5,192,900
5	14,600	19,300	43,400	115,500	291,300	654,200	1,663,800	2,803,300	5,655,700
6	14,700	19,400	43,900	116,400	298,200	707,400	1,674,600	2,820,300	5,754,000
7	14,800	19,400	43,900	117,600	301,200	723,300	1,690,500	2,911,100	5,918,000
8	14,900	19,400	44,100	118,200	302,000	731,100	1,700,200	2,947,800	6,082,400
9	14,900	19,500	45,200	119,700	302,200	744,700	1,774,600	3,001,200	6,268,100
10	15,500	19,700	45,700	122,900	302,800	765,800	1,809,300	3,160,800	6,565,200
11	15,700	19,900	46,000	125,600	306,200	772,700	1,811,300	3,162,000	7,412,000
12	15,900	20,000	46,300	126,400	306,400	775,400	1,846,500	3,213,300	7,419,200
13	16,200	20,100	46,600	126,600	307,400	775,500	1,910,700	3,237,900	7,895,700
14	16,300	20,100	46,800	126,600	318,000	780,300	1,920,500	3,273,000	8,043,400
15	16,500	20,300	46,800	128,000	326,100	800,500	1,934,800	3,336,600	8,346,200
16	16,600	21,000	47,400	128,000	327,000	813,100	1,983,600	3,549,800	8,455,000
17	16,700	21,300	48,100	128,600	330,000	826,600	2,038,100	3,579,000	9,366,800
18	16,900	21,300	48,400	129,300	331,300	829,300	2,069,100	3,631,800	11,531,900
19	16,900	21,600	48,700	131,200	332,400	843,400	2,089,800	3,649,700	13,000,000*
20	17,100	21,700	49,600	131,500	333,400	847,200	2,101,000	3,666,900	13,000,000*
21	17,200	22,000	49,600	133,200	334,300	858,100	2,149,300	3,770,000	13,000,000*
22		22,500	49,800	133,500	351,200	858,300	2,160,800	3,890,400	
23		22,800	51,000	133,500	353,200	867,800	2,179,200	4,278,600	
24		22,800	51,100	135,300	354,100	873,700	2,187,500	4,326,900	
25		23,100	51,200	135,400	366,000	880,800	2,285,000	4,482,300	
26		23,200	52,300	136,700	366,200	887,400	2,308,700	4,683,700	
27		23,600	52,800	137,200	369,600	898,000	2,311,400	4,931,600	
28		23,700	53,800	137,600	375,200	907,100	2,541,800	5,499,500	
29		24,000	53,900	140,300	377,400	923,600	2,733,600	6,001,600	
30		24,600	57,400	142,300	384,400	1,118,300	4,023,600	6,894,700	

*) Indicates that the specimen did not fail.

Table 3 Statistical parameters of fatigue life obtained by the experiment

Stress S kg/mm²	Median life $\tilde{N}$	Mean life $\bar{N}$	Standard deviation of life σ_N	Coefficient of variation of life V_N	Mean log-life μ	Standard deviation of log-life σ_L	Number of specimens n
22	15,700	15,600	1,200	0.0769	4.1907	0.0338	21
21	20,700	21,100	1,800	0.0849	4.3220	0.0364	30
18	47,100	47,800	3,900	0.0824	4.6780	0.0353	30
15	128,000	126,400	10,000	0.0789	5.1005	0.0353	30
12	326,600	324,300	34,100	0.1053	5.5086	0.0460	30
10	806,800	791,900	123,000	0.1554	5.8932	0.0715	30
8	1,959,200	2,036,400	482,300	0.2368	6.2994	0.0882	30
7	3,443,200	3,658,700	1,107,800	0.3028	6.5458	0.1236	30
6.5	7,412,000	–	–	–	–	–	21

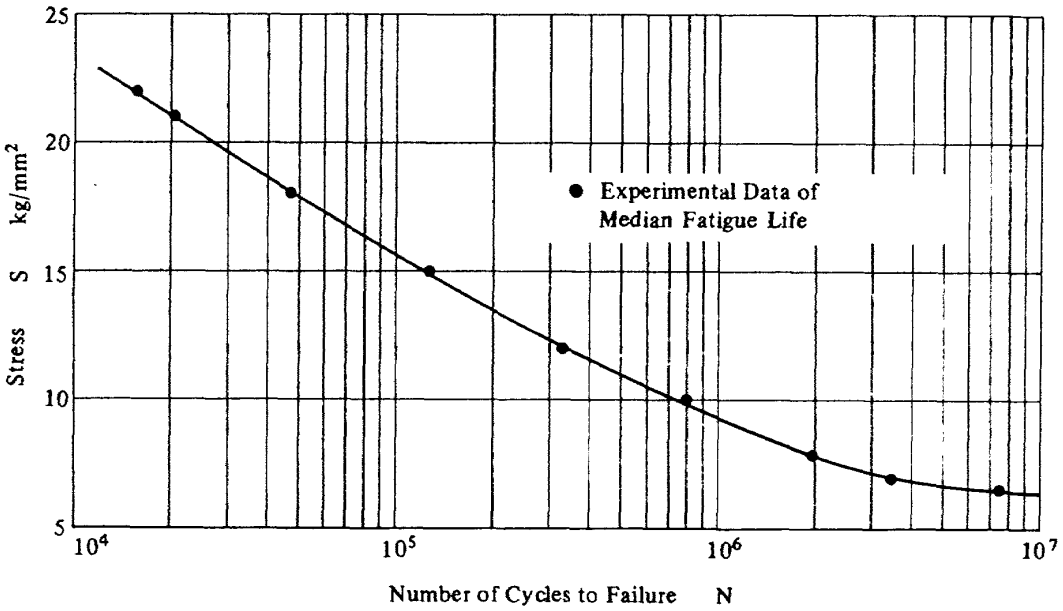

Fig. 6 $S-N$ curve for median fatigue life

Table 4 Parameters of $S-\tilde{N}$ curve and sum of squares

Stress S kg/mm²	Se	A	B	C	Sum of squares T
21	1.003×10^{1}	3.666×10^{3}	1.348×10^{4}	5.568×10^{-1}	0.298×10^{-10}
18	-1.000×10^{3}	1.051×10^{3}	-3.940×10^{3}	2.964×10^{-3}	0.362×10^{-3}
15	1.420	2.645×10^{2}	1.007×10^{4}	2.521×10^{-1}	0.142×10^{-2}
12	-1.440×10^{-1}	1.827×10^{1}	1.918×10^{4}	2.354×10^{-1}	0.137×10^{-2}
10	-5.470×10^{1}	9.832×10^{1}	-6.256×10^{4}	3.103×10^{-2}	0.612×10^{-3}
8	6.385	2.610×10^{27}	4.005×10^{6}	4.018	0.353×10^{-3}
7	6.464	3.883×10^{358}	6.205×10^{7}	4.591	0.948×10^{-8}

is determined using total five experimental $S-\widetilde{N}$ relations, i.e., at the aimed stress level and each two levels over and under it. For S = 7 and 21 kg/cm^2, the $S-\widetilde{N}$ curve equation is determined from four experimental $S-\widetilde{N}$ relations, because fatigue tests were made at one stress level under or over these stress levels. The experimental $S-\widetilde{N}$ relations are approximated with an equation proposed by Weibull[18], that is

$$S-S_e=A\,(\widetilde{N}+B)^{-C} \quad \cdots\cdots\cdots\cdots \quad (2)$$

where S_e, A, B and C are parameters. The following procedures are used to determine the four parameters. i) S_e and B are given arbitrary constants. For example, S_e and B are put zero. Any choice of initial value does not influence final results. ii) Introducing S_e and B into Eq. (3), A and C are calculated so as to make the sum of squares T_A minimum.

$$T_A=\sum_{i=1}^{m}\left\{\log(\widetilde{N}_i+B)+\frac{1}{C}\log(S_i-S_e)-\frac{1}{C}\log A\right\}^2 \quad \cdots\cdots\cdots\cdots \quad (3)$$

where m is the total number of experimental $S-\widetilde{N}$ relations used to determine the $S-\widetilde{N}$ curve equation, i.e., 5 or 4. iii) Introducing S_e, A, B and C obtained above into Eq. (4), the sum of squares T is calculated.

$$T=\sum_{i=1}^{m}\left[\log\widetilde{N}_i-\log\left\{\left(\frac{A}{S_i-S_e}\right)^{\frac{1}{C}}-B\right\}\right]^2 \quad \cdots\cdots\cdots\cdots \quad (4)$$

Moreover, iv) by changing S_e and B in steps and repeating the processes i), ii) and iii), the four parameters S_e, A, B and C are finally determined so as to make T of Eq. (4) minimum. The calculation described above is easily done using a digital computer.

The four parameters and the sum of Squares T finally obtained for each stress level are listed in Table 4. T in Table 4 shows that fairly good approximations are obtained for every stress level. The value of T at S = 18 kg/mm^2 in Table 4 is not minimum. Comparing this value to those at other stress levels, it is considered to be sufficiently small. Hence, the calculation of the parameters is suspended after this value had been obtained. Each $S-\widetilde{N}$ curve drawn by Eq. (2) and the parameters in Table 4 show a good agreement with the $S-\widetilde{N}$ curve in Fig. 6 around the aimed stress level.

4.2 Equivalent Stress Distribution Derived from Experimental Fatigue Life Distribution and $S-\widetilde{N}$ Curve

In the present paper, the accumulated effect of all factors producing the fatigue life scatter is regarded as an error in applied stress, and the error is estimated in the stress deviation from the median $S-N$ relation. Equivalent stress is defined as the sum of applied stress and the error in applied stress. Therefore, as the calculation procedure is illustrated in Fig. 7, equivalent stresses can be calculated from the experimental fatigue lives in Table 2 and the $S-\widetilde{N}$ curves determined by Eq. (2) and Table 4. The symbol S_{rA} is used for representing equivalent stress calculated as described above.

The calculated equivalent stress distributions have been plotted on normal probability paper and are shown in Fig. 8. The statistical parameters of equivalent stress are shown in Table 5. Fig. 8 apparently presents that equivalent stresses are distributed practically in a normal distribution at every stress level. The standard deviation of equivalent stress, σ_{SrA}, in Table 5 is considerably small and nearly constant irrespective of stress level. Therefore, the coefficient of variation of equivalent stress, V_{SrA}, in Table 5 becomes larger as stress level lower. The value of V_{SrA} ranges from that of static tensile strength to a little higher than it.

The facts ascertained here about the equivalent stress distribution show that an $S-\widetilde{N}$ curve plays an important role on the distribution property of fatigue life.

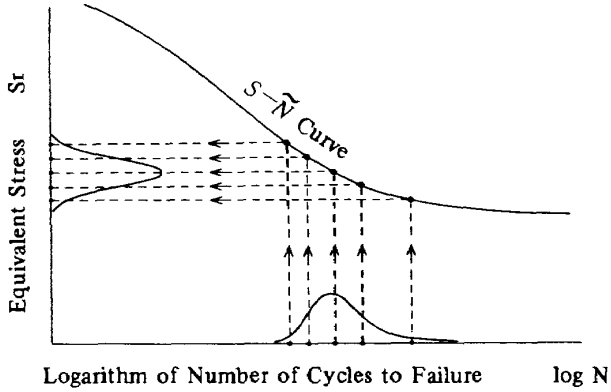

Fig. 7 Calculation procedure of equivalent stresses from experimental results

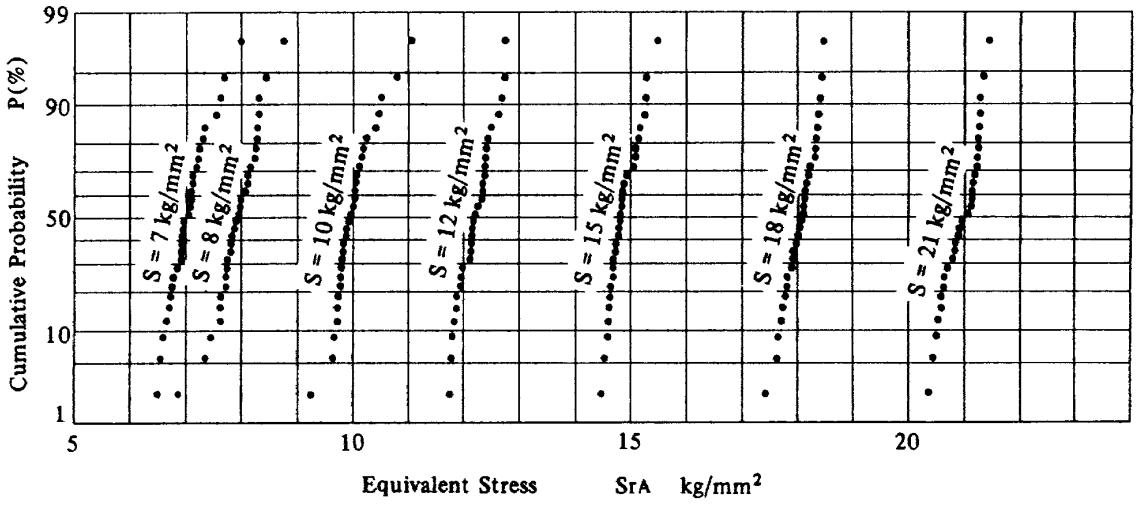

Fig. 8 Equivalent stress distributions

Table 5 Statistical parameters of equivalent stress

Stress S kg/mm²	Mean SrA kg/mm²	Standard deviation σsrA kg/mm²	Coefficient of variation VsrA
21	20.94	0.310	0.0148
18	18.05	0.267	0.0148
15	14.86	0.256	0.0172
12	12.20	0.291	0.0238
10	10.00	0.363	0.0364
8	7.93	0.375	0.0472
7	7.04	0.348	0.0494

4. 3 Fatigue Life Distribution Derived from an Equivalent Stress Distribution Model and $S-\widetilde{N}$ Curve

In this section an equivalent stress distribution model is assumed, fatigue lives are derived from this model and the $S-\widetilde{N}$ curve as illustrated in Fig. 9, and the scatter and distribution shape of fatigue life derived are discussed. It is shown in a former section that the distribution shape of equivalent stress is almost normal and its standard deviation is nearly constant regardless of stress level. Hence, the equivalent stress distribution model is assumed as follows: the distribution shape of equivalent stress is normal and its standard deviation is constant regardless of stress level. Equivalent stress is denoted by S_{rB} in this section, and its mean by $\overline{S_{rB}}$. The mean coincides with the median in a normal distribution. The standard deviation of S_{rB} is notified by

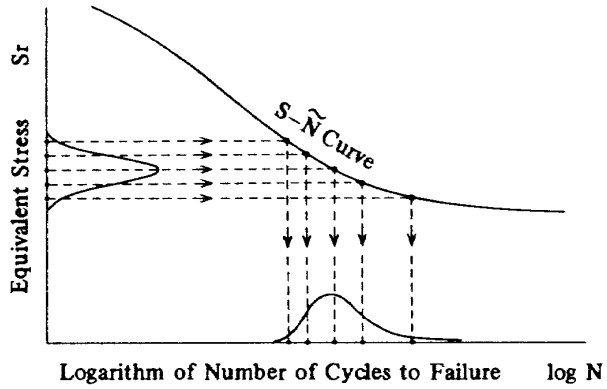

Fig. 9 Calculation procedure for fatigue life distribution from the equivalent stress distribution model

σ_{SrB}, which is considered to represent the scatter of the error in applied stress described in the Introduction and the section 4. 2.

4. 3. 1 Theoretical fatigue life distribution in the case of infinite sample size

The probability density function of equivalent stress $p(S_{rB})$, is given by

$$p(S_{rB}) = \frac{1}{\sqrt{2\pi}\,\sigma_{S_{rB}}} \exp\left\{-\frac{(S_{rB}-\overline{S_{rB}})^2}{2\sigma_{S_{rB}}{}^2}\right\}$$
$$(S_e < S_{rB} < A\cdot B^{-c}+S_e) \quad \cdots\cdots (5)$$

The relation between S_{rB} and N is provided in Eq. (2). Hence, the fatigue life N_s corresponding to $\overline{S_{rB}}$ is given by

$$N_S = \left(\frac{A}{\overline{S_{rB}} - S_e}\right)^{1/c} - B \quad \cdots\cdots\cdots\cdots (6)$$

The relation between the probability density function of theoretical fatigue life, $f(N)$, and that of equiva lent stress, $p(S_{rB})$, is as follows

$$f(N)\,dN = -p(S_{rB})\,dS_{rB} \quad \cdots\cdots\cdots (7)$$

From Eqs. (2), (5), (6) and (7), $f(N)$ is given by

$$f(N) = \frac{AC(N+B)^{-(c+1)}}{\sqrt{2\pi}\;\sigma_{S_{rB}}} \exp\left\{-\frac{\{(N+B)^{-c}-(N_S+B)^{-c}\}^2}{2\,(\sigma_{S_{rB}}/A)^2}\right\}$$

$$(0 < N < \infty) \quad \cdots\cdots\cdots\cdots (8)$$

On the other hand, the region where the S–$\widetilde{N}$ curve is considered to be a straight line is observed in Fig. 6. The S–$\widetilde{N}$ curve in this region can be represented by Eq. (9), i.e., a straight line on semilogarithmic graph paper.

$$S = -a \log \widetilde{N} + b \quad \cdots\cdots\cdots\cdots\cdots (9)$$

where a and b are positive constants. Applying the same procedure used for deriving Eq. (8), the probability density function of $\log N$, that is $g(\log N)$, is given by,

$$g(\log N) = \frac{1}{\sqrt{2\pi}\,(\sigma_{S_{rB}}/a)} \exp\left\{-\frac{(\log N - \overline{\log N})^2}{2\,(\sigma_{S_{rB}}/a)^2}\right\}$$
$$\cdots\cdots\cdots\cdots (10)$$

where

$$\overline{\log N} = (b - \overline{S_{rB}})/a \quad \cdots\cdots\cdots\cdots (11)$$

is the mean of $\log N$. Eq. (10) shows that fatigue lives in this region are distributed in a Log-normal distribution.

When sample size is infinite, the theoretical fatigue life distribution can be discussed by Eq. (8) or (10). While the sample size tested in this paper was finite, the discussion with regard to the theoretical distribution of fatigue life should be changed in a case of finite sample size. This is dealt with in the next section.

4. 3. 2 Theoretical fatigue life distribution in a case of finite sample size

In general, a fatigue life distribution obtained by an experiment is considered to be only a sample from a population. It does not hold any theoretical universality. Therefore, a finite number of equivalent stresses determined by the equivalent stress distribution model ought to have theoretical universality. It is assumed that each equivalent stress is selected as the median of order statistics. The reasons why the median of order statistics is used here are the same as those from which the median ranks were selected for the plotting method in the section 3. 2 and the S–N curve was drawn by the median fatigue lives in the section 4. 1.

Let the mean equivalent stress $\overline{S_{rB}}$ be a test stress level. The standard deviation $\sigma_{S_{rB}}$ which is calculated from a finite number n of equivalent stresses is assumed to be equal to the mean of $\sigma_{S_{rA}}$(0.316 kg/mm^2) in Table 5. Hence, the *i-th* order equivalent stress S_{rBi} at any test stress level is given by Eq. (12).

$$S_{rBi} = \overline{S_{rB}} + t_i\,\sigma_{S_{rB}} \sqrt{\frac{n-1}{\sum_{i=1}^{n} t_i{}^2}} \quad \cdots\cdots\cdots (12)$$

where t_i is the standard normal variate corresponding to the *i-th* order median rank. Sample size n is substituted by 30 which is the number of specimens tested at one stress level. As mentioned above, the equivalent stress distribution model in a case of finite sample size is defined.

As illustrated in Fig. 9, the theoretical fatigue life distribution can be calculated from the equivalent stress distribution model and the S–$\widetilde{N}$ curve determined by Eq. (2) and Table 4. The fatigue life distributions calculated are shown in Fig. 10, plotting on log-normal probability paper, and their statistical parameters are listed in Table 6. For S = 7 kg/mm^2, only the median fatigue life is listed in the Table, because the longest fatigue life was calculated to be infinite. As Fig. 10 shows, for high stress range where the S–$\widetilde{N}$ curve in Fig. 6 is practically linear, the distribution shape of fatigue life is considered to be log-normal. This is also clarified by Eq. (10). On the other hand, where the S–$\widetilde{N}$ curve exhibits downward curvature, i.e., in low stress range, the distribu-

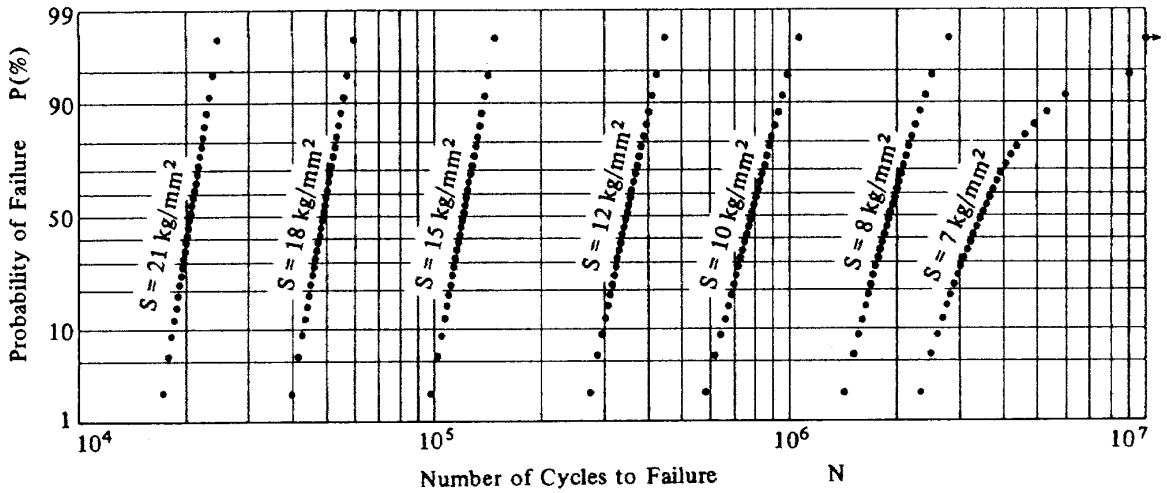

Fig. 10 Fatigue life distributions calculated from the equivalent stress distribution model and the $S-\tilde{N}$ curve

Table 6 Statistical parameters of fatigue life calculated from the equivalent stress distribution model and the $S-\tilde{N}$ curve

Stress S kg/mm²	Median life $\tilde{N}$	Mean life $\bar{N}$	Standard deviation of life σ_N	Coefficient of variation of life V_N	Mean log-life μ	Standard deviation of log-life σ_L
21	20,700	20,700	1,800	0.0856	4.3148	0.0372
18	48,400	48,600	4,700	0.0963	4.6847	0.0417
15	120,400	121,000	12,100	0.1003	5.0809	0.0434
12	347,300	350,000	41,000	0.1171	5.5412	0.0507
10	780,400	789,300	114,700	0.1453	5.8928	0.0628
8	1,899,700	1,935,600	304,700	0.1574	6.2818	0.0670
7	3,444,100	—	—	—	—	—

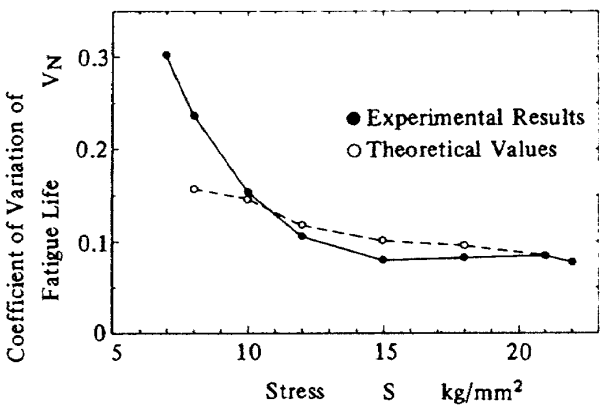

Fig. 11 Coefficient of variation of fatigue life

tion shape of fatigue life departs from the log-normal type, and its skew is pronounced. However, because the standard deviation of equivalent stress assumed in the model is comparatively small, the distribution shape of fatigue life has a tendency to form the log-normal type. The lower tail of a skewed fatigue life distribution in Fig. 10 fits well a one-sided censored log-normal distribution. This agrees well with the results of a large scale fatigue test (the total number of specimens tested at one stress level was 973) by Bloomer and Roylance[20] and gives a theoretical basis to estimate the lower tail of a fatigue life distribution which is important for probabilistic machine or structure design. The distribution tendency of fatigue life illustrated in Fig. 10 agrees well with that obtained by the experiment in Fig. 5.

To compare the calculated scatter of fatigue life with that observed, the coefficient of variation of fatigue life in Table 3 and Table 6 is shown in Fig. 11. Both values of calculated and observed agree well, except for the case of S = 8 kg/mm². The longest fatigue life at S = 8 kg/mm² in the experiment seems

to be longer than expected as the median of order statistics.

It became clear by the above discussion that the proposed equivalent stress distribution model provides a good explanation for the experimental results of fatigue life distribution within the interpolated region of the $S-\widetilde{N}$ curve drawn from the experimental results.

5. CONCLUSIONS

All factors producing fatigue life scatter were regarded as an error in applied stress. Equivalent stress was defined as the sum of applied stress and the error. This concept was used for analyzing the results of a series of fatigue tests on 2024-T4 aircraft structural aluminum alloy specimens with a sharp notch (K_t = 8.25) under a constant temperature and humidity condition. The interrelationship between scatter of equivalent stress, $S-\widetilde{N}$ curve and fatigue life scatter was discussed. The conclusions are summarized below.

1) The microscopical observations indicated that a fatigue crack grew throughout most of the whole life of a specimen, when an applied stress was higher than or equal to 8 kg/mm², while an applied stress was not higher than 7 kg/mm², the fatigue life was covered by the two periods of fatigue crack initiation and propagation. Nevertheless, there was no significant difference in the distribution shape and scatter of fatigue life between the two stress ranges.
2) The scatter of fatigue life obtained in this experiment was much smaller than many other fatigue test results.
3) The distribution shape of equivalent stress was found to be practically normal. The standard deviation was nearly constant (0.256 to 0.375 kg/mm²) regardless of stress level, and the coefficient of variation ranged from 0.0148 to 0.0494.
4) The proposed model of equivalent stress distribution, which has a normal distriburion with a constant standard deviation regardless of stress level, gave a good explanation of the experimental fatigue life distributions within the interpolated region of the $S-\widetilde{N}$ curve drawn from the experimental results.
5) The following facts were verified experimentally and theoretically. In the stress range where the $S-\widetilde{N}$ curve on semilogarithmic graph paper is practically linear, the distribution shape of fatigue life is considered to be log-normal. On the other hand, where the $S-\widetilde{N}$ curve exhibits downward curvature, the distribution shape of fatigue life departs from the log-normal type and its skew is pronounced. However, because the standard deviation of equivalent stress obtained in this study is comparatively small, the distribution of fatigue life has a tendency to form the log-normal type.

ACKNOWLEDGMENTS

The authors are deeply indebted to Professor Sakae Tanaka and Lecturer Satoshi Akita of the University of Electro-Communications for their valuable suggestions and encouragement during this research. Thanks are due also to Tadao Kamiyama, former Senior Scientific Research Officer, Eiichi Nakai, Head of the Second Airframe Division, and Soshiro Iida, Chief of the Fatigue Section, of the National Aerospace Laboratory for their kind discussions on this work.

REFERENCES

1) T. Yokobori; Strength, Fracture and Fatigue of Materials, P. Noordhoff, Goningen, Netherlands, 1965.
2) T. Shimokawa and Y. Hamaguchi; Relation Between Scatter of Fatigue Life and S–N Curve in Aircraft Structural Aluminum Alloy 2024-T4, Journal of the Japanese Society for Strength and Fracture of Materials, Vol. 9, No. 3, 1974, pp. 1 ~ 12, and Technical Report of National Aerospace Laboratory, TR-360, 1974.
3) M. Matolcsy; Logarithmic Rule of Fatigue Life Scatters, Materialprüfung, Vol. 11, No. 6, 1969, pp. 196 ~ 200.
4) S. Tanaka and S. Akita; On the Miner's Damage Hypothesis in Notched Specimens with Emphasis on Scatter of Fatigue Life, Engineering Fracture Mechanics, Vol. 7, No. 3, 1975, pp. 473 ~ 480.
5) M. Isida; Proceedings of the Symposium on

Fracture Mechanics, 1971, pp. 6-1 ~ 6-64.

6) L. G. Johnson; Statistical Treatment of Fatigue Experiments, Elsevier Publishing Comp., 1964.

7) Z. Yamauti, et al., eds.; Statistical Tables and Formulas with Computer Applications, Japanese Standards Application, 1972.

8) G. M. Sinclair and T. J. Doran; Effect of Stress Amplitude on Statistical Variability in Fatigue Life of 75S-T6 Aluminum Alloy, Trans. ASME, Vol. 75, 1953, pp. 867 ~ 872.

9) A. M. Freudenthal and E. J. Gumbel; On the Statistical Interpretation of Fatigue Tests, Proc. Roy. Soc. (London), A-216, 1953, pp. 309 ~ 332.

10) I. Konishi and M. Shinozuka; Scatter of Fatigue Life of Structural Steel and Its Influence on Safety of Structure, Memoirs of the Faculty of Engineering Kyoto University, Vol. 18, 1956, pp. 73 ~ 83.

11) H. T. Corten and G. M. Sinclair; A Wire Fatigue Machine for Investigation of the Influence of Complex Stress Histories, Proc. ASTM, Vol. 56, 1956, pp. 1124 ~ 1137.

12) M. Kawamoto, T. Nakagawa, Y. Ibuki and T. Takahashi; Statistical Distribution of the Fatigue Life of Steel and the Effect of Heat-Treatment on the Dispersion of the Fatigue Life, Journal of the Society of Materials Science, Japan, Vol. 9, No. 87, 1960, pp. 736 ~ 741.

13) T. Yokobori, I. Maekawa and S. Korekawa; The Influence of Non-Metallic Inclusions on the Fatigue Strength and the Statistical Nature of Steel, Journal of the Society of Materials Science, Japan, Vol. 12, No. 117, 1963, pp. 434 ~ 438.

14) M. Isida and T. Koono; Rotating Bending Fatigue Test on Unnotched Bar Specimens of 2024-T4 Aluminum Alloy, Technical Memorandum of National Aerospace Laboratory, TM-56, 1965.

15) M. Sano and K. Komooka; Plain Bending Fatigue Test on Sheet Specimen with a Center Hole of 2024-T4 and 7075-T6 Aluminum Alloy and Axial Loading Fatigue Test on Unnotched Bar Specimen of 2024-T4 Aluminum Alloy, Technical Memorandum of National Aerospace Laboratory, TM-96, 1966.

16) S. Tanaka and S. Akita; Statistical Aspects of Fatigue Life of Metals under Variable Stress Amplitudes, Trans. JSME, Vol. 38, No. 313, 1972, pp. 2185 ~ 2192.

17) H. W. Liu and H. T. Corten; Fatigue Damage under Varying Stress Amplitudes, NASA TN D-647, 1960.

18) W. Weibull; Fatigue Testing and the Analysis of Results, Pergamon Press, 1961.

19) T. Kamiyama; Design for Structural Reliability, Journal of the Japan Society for Aeronautical and Space Sciences, Vol. 19, No. 204, 1971, pp. 8 ~ 15.

20) N. T. Bloomer and T. F. Roylance; A Large Scale Fatigue Test of Aluminum Specimens, The Aeronautical Quartery, Vol. 16, No. 4, 1965, pp. 307 ~ 322.

TECHNICAL REPORT OF NATIONAL
AEROSPACE LABORATORY
TR-412T

航空宇宙技術研究所報告412T号(欧文)

昭和52年10月発行

発行所　航空宇宙技術研究所
東京都調布市深大寺町1,880
電話 武蔵野三鷹(0422)47-5911(大代表)
印刷所　株式会社　共進
東京都杉並区久我山4-1-7(羽田ビル)

Published by
NATIONAL AEROSPACE LABORATORY
1,880 Jindaiji, Chōfu, Tokyo
JAPAN